Adsorption of cubic liquid crystalline nanoparticles on model membranes†

Pauline Vandoolaeghe,*[a] Adrian R. Rennie,[b] Richard A. Campbell,[a] Robert K. Thomas,[c] Fredrik Höök,[d] Giovanna Fragneto,[e] Fredrik Tiberg[f] and Tommy Nylander[a]

Received 30th January 2008, Accepted 1st July 2008
First published as an Advance Article on the web 12th August 2008
DOI: 10.1039/b801630e

The interactions of lipid based cubic liquid crystalline nanoparticles (Cubosome®) with surface supported model membranes constituted of dioleylphosphatidylcholine (DOPC) have been studied *in situ* by use of ellipsometry, quartz crystal microbalance with dissipation monitoring and neutron reflectivity. The systems investigated were cubic phase dispersions of glycerol monooleate (GMO) stabilised by a non-ionic block copolymer, Pluronic® F-127. The interaction between the cubic nanoparticles and the lipid bilayer is a dynamic process where the nanoparticles initially adsorb at the bilayer surface. Interfacial lipid exchange takes place where GMO is delivered into the bilayer and DOPC is extracted into the nanoparticle (34% loss). A subsequent release of the adsorbates can be triggered when the solution concentration exceeds 0.002 mg ml^{-1}. The release shows that the attractive interaction between the cubic nanoparticles and lipid bilayer is unstable after sufficient exchange of material takes place. This instability is indicative of a local phase separation at the interface between the bilayer and the nanoparticles, which causes desorption of nanoparticles. Some particles remain attached to the bilayer even hours after the initial interaction. The ability to trigger the release of the nanoparticles through increasing the solution concentration offers exciting potential in the design of drug delivery aids.

Introduction

Self-assembled lipid structures have a large potential as delivery systems in pharmaceutical, food and cosmetic applications. Cubic phases are very promising in this perspective,[1] and they have been extensively studied[2–8] because of their high capability to solubilise lipophilic drugs and encapsulate water soluble compounds. Lipid structures can include peptides and proteins in aqueous confinements of the cubic phase, and thus retard enzymatic degradation and control the release of drugs. The use of such self-assembled structures for oral delivery of insulin has been demonstrated by Chung *et al.*[9] The challenge is to formulate liquid crystalline phases as well-defined dispersions with controllable particle size so that they can be used in, *e.g.* intravenous, oral and nasal drug delivery. Stable colloidal dispersions of the cubic liquid crystalline phase provide this possibility and have thus opened up exciting new opportunities for applications.[10,11] Moreover, new lipid compositions and processing methods have been developed that make it possible to control the particle size, morphology and stability of these nanoparticles.[12,13]

The adsorption of these dispersions on bare surfaces has been studied previously,[14] and the interaction is very strongly dependent on the surface properties. These properties are dependent on the solution conditions such as pH or presence of electrolytes, which also affect the stability of the nanoparticles. The interaction of the liquid crystalline nanoparticles with a membrane is important for the fundamental understanding of the uptake of the drugs and the fusogenic properties of the delivery system.

Phospholipid bilayers have been used extensively as model membranes on silica surfaces, and they can be prepared in several different ways, with vesicle fusion, Langmuir–Blodgett and Langmuir–Schaeffer techniques being the most commonly used.[15,16] Another option to bring the phospholipids to the surface is *via* co-adsorption, where the phospholipids are solubilised with a surfactant, *e.g.* maltoside.[17] This method is based on gradual approach of the two-phase region of the dioleolyphosphatidylcholine (DOPC)–dodecyl dimaltoside (DDM) aqueous system, which results in the deposition of a dense lipid bilayer structure.

The present study concerns the adsorption to a DOPC bilayer and subsequent interfacial processes of cubic phase nanoparticles (CPNPs) with the trade name Cubosome®, which are based on glycerol monooleate (GMO) and stabilised by a non-ionic block copolymer, Pluronic® F-127. The GMO aqueous phase behaviour is well characterised, and it has been shown that with increasing water content reverse micellar (L_2), lamellar (L_α) and two types of bicontinuous reverse cubic (V_2) liquid crystalline phases are formed at room temperature.[18,19] The *in situ* methods used are null ellipsometry, quartz crystal microbalance with

[a]*Department of Physical Chemistry 1, Lund University, Box 124, SE-221 00 Lund, Sweden. E-mail: Pauline.Vandoolaeghe@fkem1.lu.se; Fax: +46 46222 4413; Tel: +46 46222 3332*
[b]*Department of Physics, Uppsala University, Box 530, SE-751 21 Uppsala, Sweden*
[c]*Physical & Theoretical Chemistry Laboratory, University of Oxford, South Parks Road, Oxford, United Kingdom OX1 3QZ*
[d]*Division of Solid State Physics, Lund University, Box 118, SE-221 00 Lund, Sweden*
[e]*Institut Laue-Langevin, 6 rue Jules Horowitz, BP 156, 38042 Grenoble Cedex 9, France*
[f]*Camurus AB, Ideon Science Park Gamma 1, SE-223 70 Lund, Sweden*
† Electronic supplementary information (ESI) available: Null ellipsometry data for the formation of the DOPC bilayer, and QCM-D data for both the formation of the DOPC bilayer and the interaction of the CPNPs with the bilayer. See DOI: 10.1039/b801630e

dissipation monitoring (QCM-D) and neutron reflectivity. As an optical technique with a time resolution on the order of seconds, null ellipsometry allows us to study the evolution of the adsorbed amount and thickness. As a complementary acoustic technique with a similar acquisition rate, QCM-D allows us to determine the 'wet mass', *i.e.* the 'dry mass' (or optical mass) that can be derived from ellipsometry plus the contribution from coupled water molecules. Neutron reflectivity scans were acquired for at least one hour, which placed a strong limitation on the kinetic information available. Its importance instead came from insight gained into the composition and structure of the adsorbed layers, through exploiting isotopic substitution of the phospholipid bilayer and of the solution phase.

Experimental section

Materials

Glycerol monooleate that contains a small amount of diglycerides (44 : 1 weight ratio; RYLO™ MG19, Lot No. 2119/65-1) was provided by Danisco Ingredients (Brabrand, Denmark). The fatty acid composition was 89.3% oleic, 4.6% linoleic, 3.4% stearic and 2.7% palmitic acid. A triblock copolymer containing ethylene oxide (EO) and propylene oxide (PO) groups, with the trade name Pluronic® F-127, and an approximate formula of $EO_{98}PO_{57}EO_{98}$ (average molecular weight of 12 600 g mol^{-1}) was obtained from BASF Svenska AB (Helsingborg, Sweden).

Sterile water from B. Braun Medical AB (Bromma, Sweden) was used for the preparation of the CPNP stock solution. All other solutions were prepared with MilliQ water (a resistivity of 18 MΩ cm and a total organic content of 3–4 ppb).

Dioleylphosphatidylcholine (DOPC) was purchased from Avanti Lipids (Alabaster, USA) and *n*-dodecyl-β-D-maltopyranoside (DDM) from Anatrace (Maumee, Ohio, USA). Dioleylphosphatidylcholine with perdeuterated acyl chains (d-DOPC) was synthesised in the group of Prof. Eugenijus Butkus at the Department of Organic Chemistry, Vilnius University, Lithuania by esterification of the glycerophosphatidylcholine cadmium salt with fully deuterated oleic acid, which in turn was synthesised at the Physical and Theoretical Chemistry Laboratory, University of Oxford, UK.

Acidic solutions were prepared by dilution of concentrated HCl purchased from Merck. All chemicals were used as received.

Preparation of the CPNPs

Coarse dispersions of CPNPs were prepared by adding melted (40 °C) GMO into F-127 solution. In all experiments, the lipid : polymer ratio was 9 : 1 (w/w). The sample volume was typically 50–200 ml. The samples were immediately sealed, vigorously shaken and then left to vortex for 24–48 hours on a mechanical mixing table at ~300 rpm at room temperature. The resulting coarse dispersions were homogenised by passing the solution 5–8 times through a Microfluidizer 110S (Microfluidics Corp., Newton, USA) at 345 bar and 25 °C. The subsequent heat treatment was performed using a bench-type autoclave (Certo-Clav CV-EL, Certoclav Sterilizer GmbH, Traun, Austria) operating at 125 °C and 1.4 bar vapour pressure. The samples were transferred into Pyrex glass bottles (50–500 ml) and put into an autoclave. A period of about 12 min was required to vent the entrapped air and to heat up the autoclave. The samples were subjected to heat treatment for 20 min at 125 °C, then allowed to cool to room temperature before analysis. The dispersions were filtered through a 2 μm Acrodisc® syringe filter (Pall Corp., Ann Arbor, USA) to remove small amounts of large precipitates formed during cooling at the air/liquid interface.

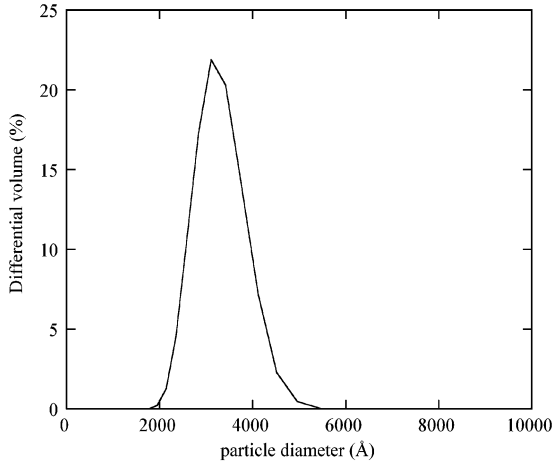

Fig. 1 Particle size distribution of the cubic phase nanoparticle dispersions measured by a laser diffraction particle size analyzer.

The internal structure of the cubic particles obtained has the body-centered cubic space group *Im*3*m* (No 229).[13]

The particle size distribution was measured using a Coulter LS230 laser diffraction particle size analyzer (Beckman-Coulter, Inc., Miami, USA), which operates on the principles of Fraunhofer diffraction for large particles (0.4–2000 μm) and uses the polarisation intensity differential scattering (PIDS) method for small particles (0.04–0.5 μm). The instrument was fitted with a volume module (125 ml). Data were collected for 90 s. A standard model based on homogeneous oil spheres with a refractive index of 1.46 was used for the particle size calculations. Reasonable estimates of the uncertainty in the refractive index can only shift the obtained particle diameter distribution by a few percent. Note that the model is based on spherical particles and the measured mean particle size is calculated based on this assumption. Fig. 1 shows that the mean diameter of the nanoparticles was 3400 Å with a polydispersity index of 0.16. This index is defined as the ratio between the standard deviation and the mean size. The volume of water in the particles is estimated to ~45% using the following equation:[20,21]

$$\phi_l = 2A_0\left(\frac{l}{a_{cub}}\right) + \frac{4\pi\chi}{3}\left(\frac{l}{a_{cub}}\right)^3 \quad (1)$$

where ϕ_l is the volume fraction of the lipid, l the thickness of the monolayer (17 Å), a_{cub} the lattice parameter (135–140 Å), A_0 the ratio of the area of the minimal surface in a unit cell to its volume to the power of 2/3 (2.345 for No 229), and χ the Euler characteristic of the surface (–4 for No 229).

Ellipsometry

Instrument. An automated Rudolph Research thin-film null ellipsometer, type 43603-200E was used to measure the adsorbed

amount and thickness of adsorbed layers *in situ* using the methodology described by Tiberg and Landgren.[22] The light source for these measurements was a xenon arc lamp fitted with a filter for a wavelength of 4015 Å, and the angle of incidence was 68.23°. The ellipsometer was fitted with a 5 ml cuvette, which was thermostated to 25.0 ± 0.1 °C and agitated with a magnetic stirrer at about 300 rpm.

Preparation of the substrates. The silica surfaces were provided by Stefan Klintström (Department of Chemistry, IFM, Linköping University, Sweden). Silicon wafers ((100) crystal plane, p-type, boron-doped, resistivity 1–20 Ω cm) were thermally oxidised in an oxygen atmosphere at 920 °C for about 1 hour, followed by annealing and cooling in an argon flow. This procedure yields a SiO_2 layer thickness of ~300 Å. The oxidised wafers were cut into slides with a width of 12 mm, and were cleaned in a mixture of 25% NH_4OH (pro analysi, Merck), 30% H_2O_2 (pro analysi, Merck) and H_2O (1 : 1 : 5 by volume) at 80 °C for 5 min, followed by a mixture of 32% HCl (pro analysi, Merck), 30% H_2O_2 (pro analysi, Merck) and H_2O (1 : 1 : 5 by volume) at 80 °C for 10 min.[22] The cleaned oxidised wafers were rinsed with water and ethanol and then stored in ethanol. The surfaces were dried under vacuum (0.02 mbar) and then treated in an air plasma cleaner (Harrick Scientific Corp., model PDC-3XG) for 5 min prior to the start of the experiment.

Characterisation of the substrates. The optical properties of the silica substrates, *i.e.* the complex refractive index of silicon ($\hat{n}_{Si}$), and the real refractive index (n_{SiO_2}) and thickness (d_{SiO_2}) of the oxide layer, were characterised at the beginning of each experiment. The ellipsometric angles, Ψ and Δ, were measured in two different ambient media, air and solution. Numerical calculations were performed on the four measured parameters using a three-layer stratified optical model.[23] A typical substrate characterisation was $\hat{n}_{Si} = 5.5 - 0.3i$, $n_{SiO_2} = 1.5$ and $d_{SiO_2} = 300$ Å.

The recorded values of Ψ and Δ correspond to the relative amplitude change and phase shift upon reflection of polarised light at an interface, respectively. The ellipsometric angles are related to the complex reflectivity coefficients for light components polarised parallel and perpendicular to the plane of incidence, $\hat{r}_p$ and $\hat{r}_s$, respectively:

$$\frac{\hat{r}_p}{\hat{r}_s} = \tan\Psi e^{i\Delta} \quad (2)$$

Formation of the DOPC bilayer. The supported lipid bilayer was formed on silica by adsorption and deposition from an aqueous solution of DOPC solubilised by the sugar surfactant DDM at a ratio of 1 : 6.[24,25] The bilayer formation was achieved by a series of subsequent additions of mixed DOPC–DDM solutions of decreasing total concentration, starting with 0.114 mg ml^{-1}. Each addition of the DOPC–DDM mixture was followed by a rinse with 0.1 mM HCl, which ensured removal of excess DDM. Three cycles of addition followed by rinsing have been shown to give a high bilayer coverage consisting only of DOPC.[17,26] The concentrations of the DOPC–DDM solutions in the second and third additions were 10% and 1%, respectively, of the starting value. All additions were made by injecting a small aliquot of a concentrated solution of the mixture into the cuvette, and rinsing steps were performed by circulating the solution by means of a peristaltic pump (Ole Dich Instrumentmakers ApS, Hvidovre, Denmark) for at least 15 min at a rate of 1.5 ml min^{-1}.

Addition of the CPNPs. The CPNP samples were added to the cuvette of the ellipsometer as a small aliquot of a concentrated solution, typically less than 150 μl diluted in 5 ml of HCl solution at pH 4.

Data evaluation. The Ellipsometry program,[27] based on McCrackin's approach,[28,29] was used to evaluate the data. The recorded ellipsometric angles were modelled using the substrate optical properties determined previously as well as one or two adsorption layers, which corresponded to a total of four or five layers, respectively. The model relied on the assumption of isotropic media and planar interfaces, as described in detail by Landgren and Jonsson.[23] The mean refractive index, n_f, and the thickness, d_f, of adsorption layers were calculated numerically.[30] The adsorbed amount, Γ, was calculated from n_f and d_f using de Feijter's expression:[31]

$$\Gamma = \frac{(n_f - n_0)d_f}{dn/dc} \quad (3)$$

where n_0 is the refractive index of the bulk solution and dn/dc is the refractive index increment of the adsorbed material as a function of its bulk concentration. In all the calculations of the adsorbed amount, the values $dn/dc = 0.148$ cm^3 g^{-1} for DOPC and $dn/dc = 0.169$ cm^3 g^{-1} for GMO were used.[24,32]

Quartz crystal microbalance with dissipation monitoring (QCM-D)

Instrument. QCM-D measurements were performed with a Q-SENSE E4 system, equipped with four liquid sample cells enabling the performance of four experiments in parallel. This technique is described in detail by Rodahl *et al.*[33] Measurements were performed with a continuous flow of the solution in the measurement chamber by means of a peristaltic pump (Ismatec, Zürich, Switzerland). The differences in resonance frequency, Δf, and dissipation, ΔD, of a coated silica surface compared with the bare substrate were measured at several harmonics simultaneously, typically 15, 25, 35 and 65 MHz. The working temperature was 22 °C.

Preparation of the substrates. Sensor crystals coated with SiO_2 with a resonance frequency of 5 MHz (QSX-303) were purchased from Q-Sense, Gothenburg, Sweden. They were first treated in the plasma cleaner for 10 min, then cleaned in a 1 wt% SDS solution for at least one hour, and lastly rinsed with MilliQ water then stored in ethanol. Prior to the start of the experiment, the surfaces were dried under vacuum (0.02 mbar) and then treated in the plasma cleaner for 5 min.

Formation of the DOPC bilayer/addition of the CPNPs. The same protocols were used as for ellipsometry, with the exception that all solutions were prepared at the desired final concentration and circulated at a continuous flow of 50 μl min^{-1} through the sample cell.

Data evaluation. The wet mass of DOPC bound to silica was calculated according to the Sauerbrey expression

$$\Delta m = \frac{C}{o_n}\Delta f \quad (4)$$

where $C \approx 17.7$ ng Hz^{-1} cm^{-2} for a 5 MHz crystal and o_n is the overtone number. This expression is a good approximation for rigid, thin and evenly distributed adsorbed films, such as a DOPC bilayer with low water content. However, the expression is not valid for non-rigid adsorbed films, such as those that result from the interaction of CPNPs with the DOPC bilayer, and other models have to be used. One good model is the Voigt-based representation[34] of a viscoelastic solid. In this model, the wet mass is represented by a frequency-dependent complex shear modulus G according to

$$G = G' + iG'' = \mu_f + i2\pi f\eta_f = \mu_f (1 + i2\pi f\tau_f) \quad (5)$$

where μ_f is the elastic shear modulus, η_f the shear viscosity, f the oscillation frequency and τ_f the characteristic relaxation time of the film. The changes in Δf and ΔD become

$$\Delta f = Im(\beta)/2\pi t_q\rho_q \quad (6)$$

and

$$\Delta D = -Re(\beta)/\pi f t_q\rho_q \quad (7)$$

where β is a function dependent on thickness and density of the film (and therefore on the wet mass), and on the bulk liquid density and viscosity.

Neutron reflectivity

Instrument. Neutron reflectivity experiments were carried out on the 'white beam' time-of-flight reflectometer, D17, at the Institut Laue-Langevin, Grenoble, France.[35] The sample cell consisted of a PTFE trough filled with 10 ml of solution and clamped against a silica substrate, as described elsewhere.[36,37] The cell was maintained at a constant temperature of (25 ± 2) °C by circulating water through its aluminium frame.

Each reflectivity profile was measured in the wavelength range λ = 2–20 Å at grazing incident angles of $\theta = 0.8°$ and 3°. Reflectivity profiles show the reflectivity, $R = (I - I_B)/I_0$, where I is the intensity after reflection at the sample, I_B is the intensity of the background and I_0 is the intensity of the direct beam transmitted through silicon, as a function of momentum transfer, $Q = (4\pi\sin\theta)/\lambda$. The value of I_B was determined by extrapolation of I/I_0 to high values of Q where there is negligible signal from the sample. The profile of I_0 was determined in a separate measurement for each incident angle. The data recorded at the two incident angles were combined. Only 4 tube detectors were available during this measurement period and so the usual method of evaluating background from adjacent regions on a position sensitive area detector was not available. One detector was positioned far away from the specular beam to evaluate the background. The reflectivity profiles were always essentially flat for $Q > 0.2$ Å^{-1}. The background reflectivity for the measurements in D_2O was typically 2×10^{-6}. Each exchange of the solution conditions was performed *in situ* with transfer of at least 40 ml of the new sample solution (about 4 times the sample cell volume) manually using a syringe.

Preparation of the substrates. The silica surfaces used were single crystal silicon blocks with a (111) plane on the large surface (2 cm × 5 cm × 12.5 cm) with an oxide layer of ~16 Å. The following process was carried out to make the blocks clean and hydrophilic. The blocks were first rinsed in ultra high quality (UHQ) water supplied by an Elga UHQ PS machine (same purity specifications as MilliQ water). They were soaked subsequently in a solution consisting of water, sulfuric acid (98%) and hydrogen peroxide (27.5% solution in water) mixed in a volume ratio of 5 : 4 : 1 respectively at 80 °C for 15 min. The blocks were then removed from the cleaning solution and allowed to cool for a few minutes before being quenched by immersion in UHQ water. The blocks were then placed in a stream of oxygen and exposed to ultraviolet light for 30 min. They were stored in UHQ water until use.

Characterisation of the substrates. Reflectivity profiles of the silica substrates were recorded in three different isotopic contrasts of water in order to reveal different features such as the roughness and thickness of the oxide layer. The contrasts used were pure D_2O, pure H_2O and a mixture of 59.5% by weight of H_2O in D_2O where the neutron refractive index is matched to that of silicon (contrast matched silicon; cmSi). In general, the combined fit to multiple isotopic contrasts can be used to remove ambiguities that arise from the loss of phase information in scattering experiments, and to solve uniquely the composition of multicomponent systems provided that the scattering length densities of the pure materials are known. The combined fits to all data sets gave the oxide layer thickness of 16 ± 2 Å, a scattering length density of $3.4 \pm 0.2 \times 10^{-6}$ Å^{-2}, a solvent content of 32 ± 4% and a roughness of 7 ± 2 Å. This roughness is quite high and can be explained by the fact that the surface had not been polished prior to the experiment.

Formation of the d-DOPC bilayer. The same preparation protocol as for ellipsometry and QCM-D was used, except that the lipid used was perdeuterated, and at least 40 ml of each solution was passed through the sample cell manually using a syringe. The d-DOPC–DDM mixture at the starting concentration, 0.117 mg ml^{-1}, was injected into the sample cell, and the reflectivity profile at the lower incident angle (0.8°) was monitored repeatedly until no further change was observed. A full reflectivity profile was then measured at both incident angles before rinsing and then addition of d-DOPC–DDM mixtures first at 10% then at 1% of the starting concentration, before further rinsing was carried out. The d-DOPC bilayer was then characterised both in D_2O and in cmSi.

Addition of the CPNPs. The effect of the interaction of the CPNPs with the lipid bilayer was investigated at two sequential concentrations, 0.001 and 0.05 mg ml^{-1}. The adsorption at the lower concentration was followed by recording repeated reflectivity profiles in D_2O until no further change was observed. The higher concentration was then added, and reflectivity profiles were recorded until the end of the measurement time when a profile was also recorded in cmSi to allow better characterisation of the adsorption layer.

Data evaluation. Neutron reflectivity is dependent on the variation of the scattering length density, ρ, normal to the surface. In turn, ρ depends on the chemical composition of the sample,[38]

$$\rho = \sum n_i b_i \quad (8)$$

where n_i is the isotopic number density of element i and b_i its scattering length. The molecular composition of adsorbed films can be determined by exploiting isotopic substitution with hydrogen and deuterium ($b_H = -3.74$ fm and $b_D = 6.67$ fm) in the adsorbed material and solution.

Derivation of structural information from reflectivity profiles is usually made by comparing the data with models calculated using an optical matrix formalism for reflectivity of thin layers, which has been described in detail elsewhere.[39] The reflectivity is calculated for assumed structural models of the adsorbed layer. The calculated reflectivity profile is then compared with the measured data. Computer programs were used, such as AFit (v.3.1),[40] which allows the simulation of reflectivity profiles simultaneously for different isotopic solution contrasts by varying the thickness, scattering length density, solvent volume fraction and roughness of each layer. In order to reduce the fitting parameters and to apply a physically relevant bilayer model the following constraints were applied: the bilayer was assumed to be symmetrical (*i.e.* the same scattering length density was used for the outer and inner leaflets of the bilayer), and the number of heads and tails in each leaflet was constrained to be equal. The choice of the number of sub-layers is dependent upon the extent of inhomogeneity across the interfacial region, but is always kept minimal.

The reflectivity profiles recorded after addition of 0.05 mg ml^{-1} nanoparticles feature a Bragg diffraction peak at high Q. In this case a multilayer with a well-defined repeat distance was added to the structural model. The fitting parameters used to describe the repeat structure are the thickness of the head groups and acyl chains, the number of repetitions and the area per head group.

Results and discussion

Formation of the lipid bilayer

Fig. 2 shows the evolution of the wet mass and dissipation difference as determined by QCM-D, during the sequential build-up of the supported DOPC bilayer through additions and rinses of mixed DOPC–DDM solutions. For comparison, the evolution of the adsorbed amount and thickness determined by ellipsometry is shown in Fig. S1a in the ESI.† The same qualitative trends are observed in the wet mass from QCM-D and in the adsorbed amount from ellipsometry. The amount of material from the two independent techniques agrees to 3%, which suggests that the layers formed contain a negligible amount of water. Note that the Sauerbrey equation was used for the calculation of Δm as no discrepancy was observed in Δf and ΔD for the different harmonics (see Fig. 1b in the ESI†).

The issue arises of how the DOPC is transported from the mixed micelles to the surface or the incomplete bilayer. One hypothesis is that the mixed micelles diffuse within the stagnant layer and spread at the surface, as suggested by Vacklin *et al.*[25] Such a model implies that it should be possible to detect an extended structure when the micelles are attached to the surface. We do not see such a structure with either ellipsometry or neutron reflectivity, but these methods are not sufficiently sensitive to detect a low density layer of attached micelles. Dissipation measurements by QCM-D, on the other hand, are very sensitive to such extended structures, which would appear as an increase in dissipation. Indeed Fig. 2 (and inset) shows a very sharp peak in dissipation difference during the first addition of the DOPC–DDM mixture ($t = 6$ min; marked *), which provides strong evidence for this extended structure of micelles adsorbed at the surface before collapse. A similar peak in dissipation is also observed when vesicles spread on surfaces to form bilayers.[41] In the present work, the magnitude of the peak was used to follow the spreading process. The corresponding peak is much smaller after the second addition ($t = 45$ min; marked #), and does not appear after the third addition. We reason that the micelles have less affinity to undergo direct surface adsorption as the surface becomes more highly covered with DOPC, *i.e.* as the number of layer defects decrease. These data also provide evidence that the experimental protocol is adequate to form a bilayer with high coverage.

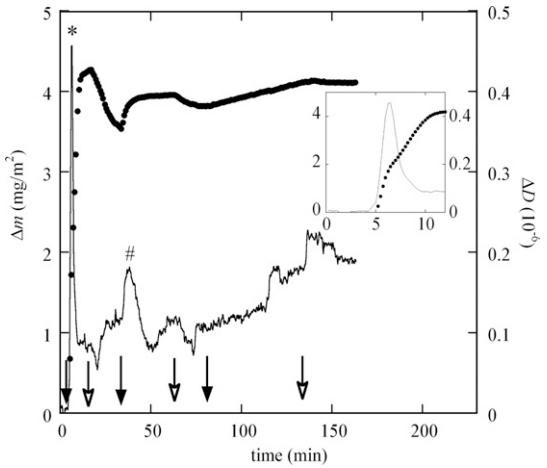

Fig. 2 Wet mass Δm (filled symbols) and dissipation difference ΔD (solid line) determined by QCM-D, with an inset showing an expansion of the first 12 minutes. The DOPC bilayer was formed by three cycles of addition followed by rinsing of DOPC–DDM mixtures, as described in the text. The times of the additions are indicated by filled arrows and the times of rinsing by open arrows. Peaks in ΔD after the first and second additions are marked with * and # symbols, respectively.

Neutron reflectivity measurements allow us to determine the composition of the layer, *i.e.* the amount of DDM that is present in the bilayer after each sequential DOPC–DDM addition. This analysis was possible using DOPC with perdeuterated chains, and therefore the presence of hydrogenated DDM was detectable with proper contrast matching of the solvent. Fig. 3 shows the reflectivity profiles and fits obtained after the first d-DOPC–DDM addition (0.117 mg ml^{-1}), and after the last rinsing step, with the bare surface data shown for comparison, both in D_2O and in cmSi. The fitting parameters obtained are summarised in Table 1.

The percentage of solvent after the first step is 30%, but the value increases to 45% by the end of the formation process. This high solvent content indicates that the final bilayer does not

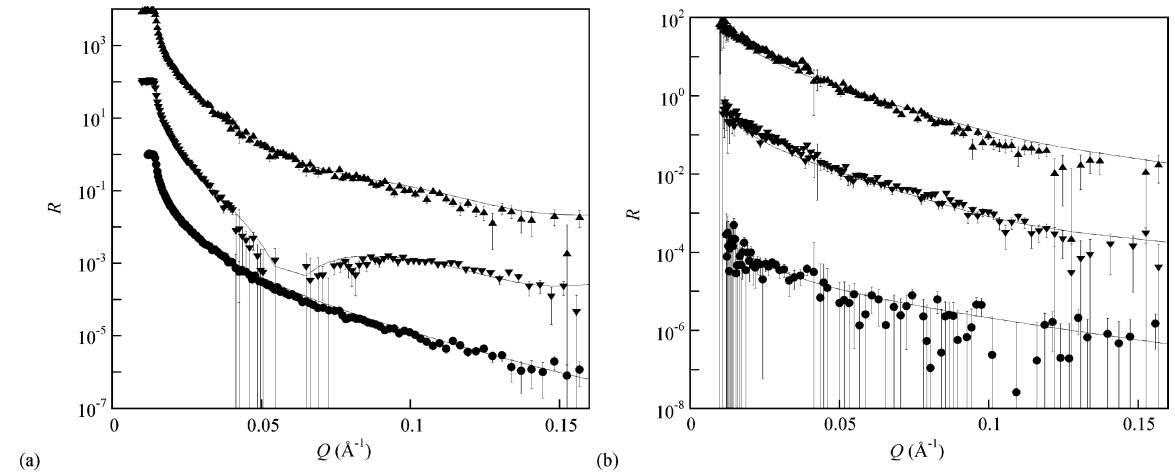

Fig. 3 Neutron reflectivity profiles (reflectivity R recorded as a function of momentum transfer Q) for a bare silica surface (circles), after addition of the mixture d-DOPC–DDM 1 : 6 (w/w) at a concentration of 0.117 mg ml^{-1} (inverse triangles; shifted up by a factor of 10^2 for clarity) and for the d-DOPC bilayer (triangles; shifted up by a factor of 10^4 for clarity). The solution contrasts were in (a) D_2O and (b) cmSi. The thin lines correspond to the fits.

Table 1 Neutron reflectivity fitting parameters for a d-DOPC bilayer obtained by the fit of the three-layer adsorption model to measurements recorded in D_2O and cmSi after the bilayer formation process was finished: 'd' is the layer thickness, 'ρ' is its scattering length density, '$\%_{solv}$' is the proportion of solvent in the layer, and 'rough' is the roughness of the layer. The numbers in parentheses correspond to the values of the parameters after the first addition of the DOPC–DDM mixture

	d/Å	$\rho 10^{-6}$ Å^2	$\%_{solv}$	rough/Å
Head groups	[7 ± 1]	[1.8 ± 0.2]	[40 ± 8]	[3 ± 1]
	7 ± 1	1.8 ± 0.2	55 ± 8	3 ± 1
Acyl chains	[29 ± 3]	[4.5 ± 0.3]	[30 ± 4]	[8 ± 2]
	29 ± 3	6.0 ± 0.3	45 ± 4	8 ± 2

completely cover the surface, and suggests that DDM was rinsed out of the partial bilayer and replaced with solvent rather than lipid. This low coverage has not been observed using ellipsometry or QCM-D, with both methods giving typical values for a well-covered bilayer. AFM has also been performed on this system[24] and showed a bilayer without defects. One possible explanation could be that the flow conditions in the neutron reflectivity sample cell, which had the highest volume of the three techniques, were different from those used with the other techniques, as it had no continuous stirring (modifications to the sample cells have since been made to address this limitation). Another possibility is that the different surface properties of the substrates affect the interfacial chemistry, as the neutron reflectivity experiment uses silica substrates with the largest surface area and lowest roughness, as well as a different crystal plane of silicon.

The obtained value of (43 ± 4) Å for the final layer thickness is consistent with that obtained by ellipsometry. The model is consistent with previous studies.[25]

Interaction of CPNPs with the lipid bilayer

The interaction between GMO-based CPNPs and DOPC bilayers is strongly dependent on the solution concentration of the particles as well as on the incubation time. Fig. 4 shows the adsorbed amount and layer thickness from ellipsometry measurements. Two different optical models were used to treat the data. Fig. 4a shows the data evaluated with a model that consists of two distinct layers of adsorbed material (two-layer adsorption model). The adsorption of CPNPs is taken to occur on top of the bilayer and the cubic particles remain intact with the bilayer unchanged. Fig. 4b shows the data evaluated with a single adsorbed layer (one-layer adsorption model) where GMO mixes with DOPC into a single layer. Fig. 4c and d show schematic representations of these models.

Different values of the refractive index increment, dn/dc, for the (inner) DOPC bilayer (0.148 cm^3 g^{-1}) and the (outer) CPNPs (0.169 cm^3 g^{-1}) were used for the two-layer adsorption model. Fig. 4a shows the adsorbed amount and thickness for the two layers combined. A value of dn/dc in between the values for DOPC and GMO was used for the one-layer adsorption model. This value is estimated from the neutron reflectivity analysis below, where the steady state composition of the layer after one hour is 42% GMO and 58% DOPC. The proportional value of dn/dc is thus 0.157 cm^3 g^{-1}. We note that the composition could be quite different before a steady state is reached, but likely differences would result in an error in the adsorbed amount of just a few percent, and the overall trends would be unaffected.

These two models represent limits of mixing and separation, which are useful to compare possible interaction mechanisms and allow us to elucidate the resulting layer structures. A drawback of the two-layer adsorption model is that if the CPNPs were not to adsorb intact, but were to interact with the lipid bilayer by collapsing, then the changes in the ellipsometric angles would be interpreted in terms of a fictional low density layer with large thickness. There is also a disadvantage of the one-layer adsorption model. If the CPNPs adsorb intact, there are two interfacial regions of very different densities which are not appropriate to model as a single mixed layer. During the adsorption process of entire CPNPs, the optical properties of the combined surface layer would change considerably. It is unrealistic to constrain the model to a bilayer with low water content.

Regardless of the details of the ellipsometry model employed, there is an initial rapid increase in adsorbed amount when adding CPNPs at a concentration of 0.05 mg ml^{-1}, before a maximum is

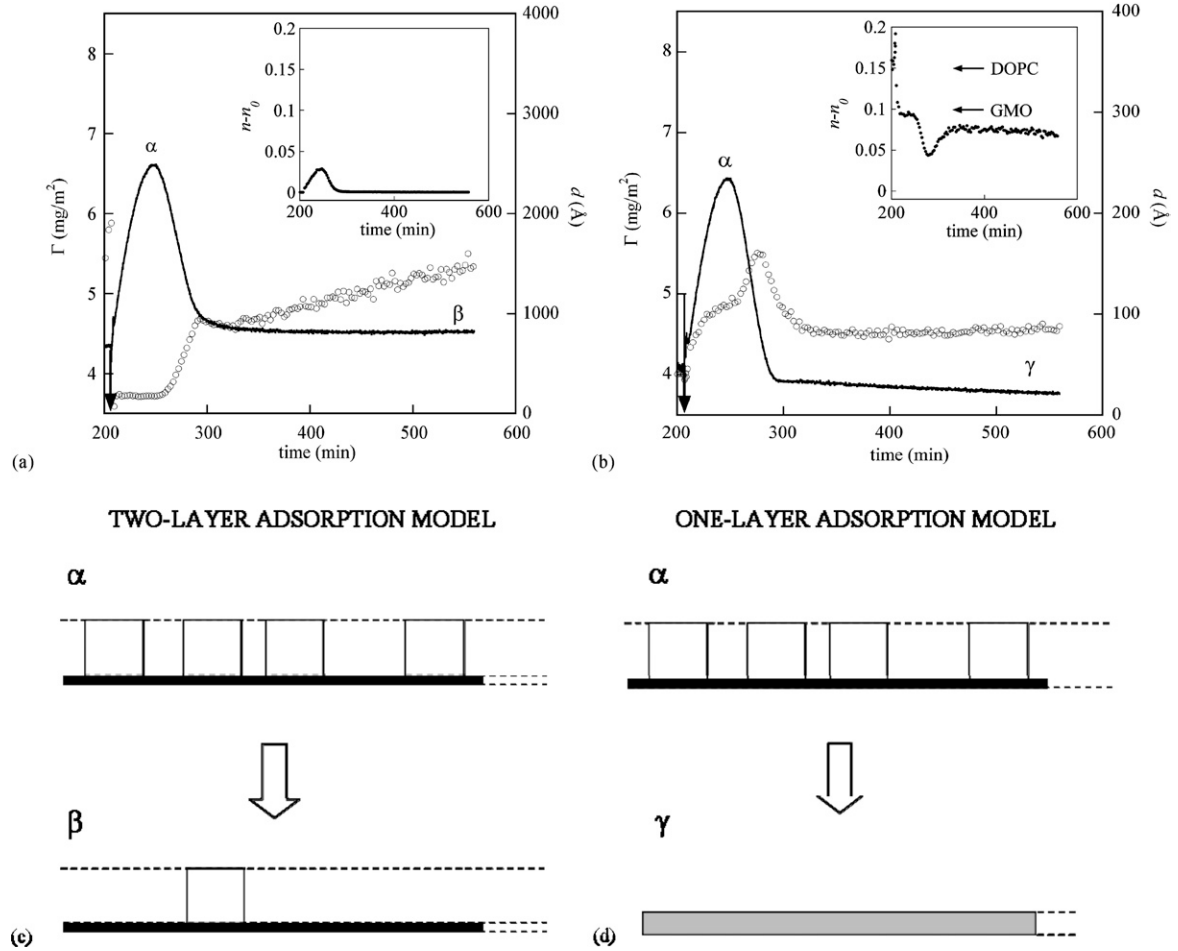

Fig. 4 Adsorbed amount Γ (solid line) and layer thickness d (open circles) determined by ellipsometry using (a) a two-layer adsorption model and (b) a one-layer adsorption model, which are shown schematically in (c) and (d), respectively, where GMO is white, DOPC is black and a GMO–DOPC mixture is grey. Schemes α, β and γ in illustrations (c) and (d) correspond to points α, β and γ in the data evaluation of plots (a) and (b). The dashed lines correspond to the stratified layers considered in ellipsometry data evaluation. All data are shown as a function of time after the addition of CPNPs at a concentration of 0.05 mg ml^{-1} to a DOPC bilayer at pH 4. The time of addition of the CPNPs is indicated by arrows.

reached at an incubation time of ~245 min (Fig. 4a and b). Note that these experiments have been repeated and show good reproducibility with $\Gamma = 6.8 \pm 0.3$ mg m^{-2} at the maximum in the adsorbed amount (standard deviation < 5%). By ~300 min there is sufficient net release of material from the interface that the total adsorbed amount has a value close to that of the lipid bilayer.

The calculated values of the thickness after 300 min are very different for the two models, but in both cases the values fall between those expected for a lipid bilayer and for a bilayer with bound CPNPs. The refractive index difference for the CPNP layer of the two-layer adsorption model (see inset in Fig. 4a) is only slightly higher than that of solution, and the thickness is close to that of the CPNPs. The refractive index difference for the one-layer adsorption model (see inset in Fig. 4b) is lower than the values for either pure DOPC or pure GMO (values indicated by arrows in the inset of Fig. 4b), and the thickness is double. The results from neither model tell the whole story, yet together they point towards the existence of a low coverage of intact CPNPs remaining at the surface hours after the initial adsorption and majority release.

Fig. 5 shows the same qualitative trends in the wet mass by QCM-D measurements as those observed in the adsorbed amount by ellipsometry. The frequency shift and dissipation difference obtained at the different harmonics of the resonance frequency are shown in Fig. S2 in the ESI.† The values of the two parameters vary for the different harmonics, which rationalises the use of the Voigt representation to model the data in this case. The value of Δm reached at the peak maximum, compared with the value of Γ calculated from ellipsometry, shows that the amount of coupled water is roughly 70%. The large dissipation change and the fact that the dissipation differs for the different harmonics (see ESI†) shows that for a period of 60 min the layer is highly viscoelastic. These findings strongly suggest that there is appreciable adhesion of intact CPNPs to the DOPC bilayer only during this initial incubation period, which is similar to the behaviour on bare hydrophilic silicon surfaces.[13] The fact that the dissipation is different for the different harmonics even when the data have reached steady state (after the net release of mass from the surface) is evidence for the presence of whole CPNPs fused to the DOPC bilayer, which supports our conclusions from ellipsometry.

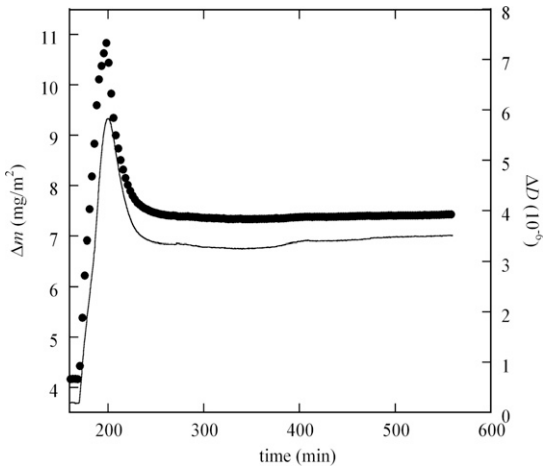

Fig. 5 Wet mass Δm (filled circles) and dissipation difference ΔD (line) determined by QCM-D, obtained using a density of 1.050 g cm^{-3} from mass-uptake estimations using Voigt-based viscoelastic modelling as a function of time after the addition of CPNPs at a concentration of 0.05 mg ml^{-1} to a DOPC bilayer at pH 4. Note that the dissipation difference is frequency dependent and the values plotted here correspond to the 3rd harmonic of the resonance frequency.

To investigate the net release of material from the surface, two ellipsometry experiments were performed in two steps each. Fig. 6a and b show the adsorbed amount and thickness evolution for the addition of a concentration of CPNPs 50 times lower than before (0.001 mg ml^{-1}) followed by addition of a concentration the same as before (0.05 mg ml^{-1}). The data treatment involves the two interfacial models described previously. Fig. 6c and 6d show the adsorbed amount and thickness for the addition of 0.001 mg ml^{-1} followed by 0.002 mg ml^{-1} using the same optical models. In each case two arrows correspond to CPNP additions.

In both experiments, for the lowest concentration of CPNPs, the adsorbed amount increases slowly to a plateau value and no net release of material is observed. Note that the values of adsorbed amount reached after addition of the low concentration are not the same for the two experiments because equilibration was not reached before the second addition in the case of Fig. 6a and b. After addition of the high concentration, 0.05 mg ml^{-1}, as before, a net release of material from the surface leads to an adsorbed amount around the same value as for the initial bilayer. These observations show that the solution concentration of CPNPs can be tuned to trigger the release of particles from the bilayer. A concentration as low as 0.002 mg ml^{-1} is the limit

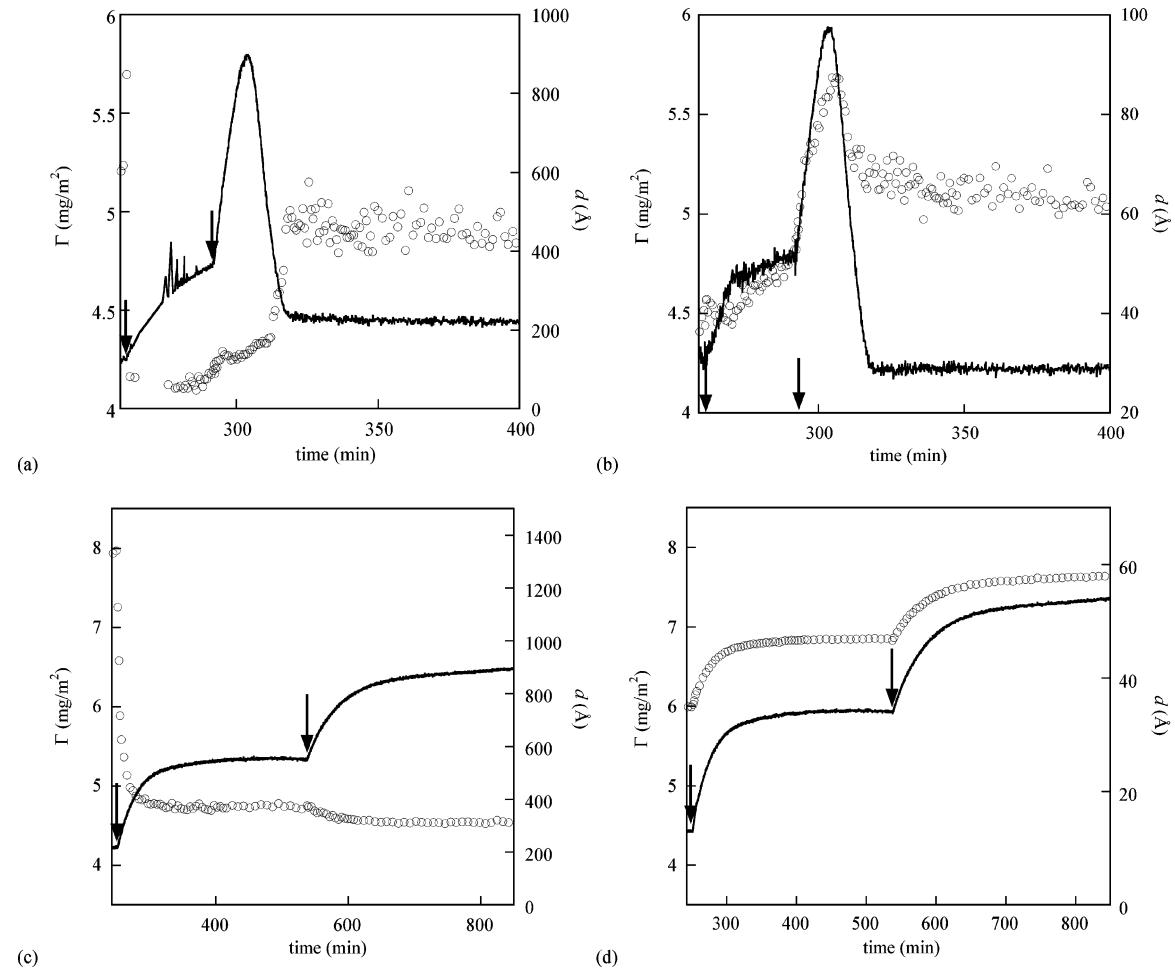

Fig. 6 Adsorbed amount (solid line) and layer thickness (open circles) determined by ellipsometry using (a,c) a two-layer adsorption model and (b,d) a one-layer adsorption model as a function of time after the addition of CPNPs at concentrations of 0.001 mg ml^{-1} then (a,b) 0.05 mg ml^{-1} (indicated by the left arrow) and (c,d) 0.002 mg ml^{-1} (indicated by the right arrow in each case) to a DOPC bilayer at pH 4.

concentration before observing the release (data not shown). The ability to stimulate release of nanoparticles bound to a lipid bilayer offers interesting scope for drug delivery applications.

The release of CPNPs from the lipid bilayer is indicative of a change in the bilayer composition that makes the interaction of particles unfavourable with the newly formed interface.

Ellipsometry and QCM-D measurements have shown us the adsorption and release mechanism, and have indicated a low coverage of residual bound CPNPs. These techniques, however, give little information about the composition of the interface, *i.e.* exchange or delivery of material, so neutron reflectivity experiments were carried out to investigate the layer structure and composition.

To recreate the sequential additions and triggered release of material observed with ellipsometry, the experiment was also performed in two steps with additions of 0.001 mg ml^{-1} then 0.05 mg ml^{-1} CPNPs into the solution phase. Fig. 7 shows five reflectivity profiles recorded over a period of 240 min after the addition of CPNPs at a concentration of 0.001 mg ml^{-1} in D_2O at pH 4. The solid lines are the fits using a three-layer adsorption model (head groups/acyl chains/head groups); Table 2 shows the fitting parameters for the thickness d and scattering length density ρ. After this time, no further changes in the reflectivity profiles were observed. Note that a three-layer adsorption model is sufficient to represent the system even if a low coverage of CPNPs adsorb on top of the bilayer. The two overlapping simulations in the inset of Fig. 7 show that there is a negligible effect on neutron reflectivity profiles if there is a thick hydrogenous layer with a surface coverage corresponding to < 7% of adsorbed CPNPs appended to the bilayer, both for cases with and without ordering of the lipid molecules into repeating layers

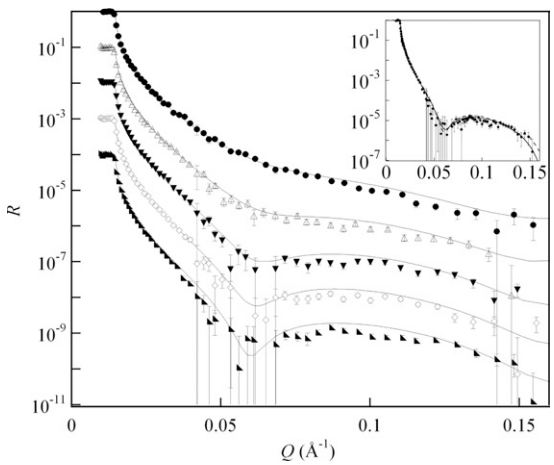

Fig. 7 Neutron reflectivity profiles and fitting curves (lines) recorded after the addition of CPNPs at a concentration of 0.001 mg ml^{-1}, after 0 min (a d-DOPC bilayer; filled circles), 15 min (open triangles), 90 min (filled inverse triangles), 165 min (open diamonds) and 240 min (filled triangles) at pH 4. For clarity, the profiles have been displaced by factors of 10. The inset reproduces the reflectivity profile recorded after 240 min and includes two overlapping simulated curves. For the simulations, the model comprises the same bilayer parameters plus a thick hydrogenous layer (2000 Å) with very high water content appended on top both with (dashed line) and without (solid line) ordering of the lipid molecules, in each case corresponding to a coverage of 7% adsorbed CPNPs.

Table 2 Neutron reflectivity fitting parameters for a d-DOPC bilayer (0 min) and for five adsorbed layers (15–315 min) after the interaction of 0.001 mg ml^{-1} CPNPs: subscripts ac and hg stand for acyl chains and head group region, respectively. The solvent volume fraction and roughness of each layer were kept the same as for the bilayer. Further definitions can be found in the caption for Table 1

Time (min)	d_{hg}/Å	d_{ac}/Å	$\rho_{hg}/10^{-6}$ Å^2	$\rho_{ac}/10^{-6}$ Å^2
0	7 ± 1	29 ± 3	1.8 ± 0.2	6.0 ± 0.3
15	7 ± 1	27 ± 2	1.8 ± 0.2	5.0 ± 0.2
90	7 ± 1	25 ± 2	1.8 ± 0.2	4.4 ± 0.2
165	7 ± 1	25 ± 2	1.8 ± 0.2	3.8 ± 0.2
240	7 ± 1	25 ± 2	1.8 ± 0.2	3.4 ± 0.3
315	7 ± 1	25 ± 2	1.8 ± 0.2	3.4 ± 0.3

(see the text below about the analytical approach of modelling repeating multilayers of lipids). The technique as set up during this experiment will thus not be sensitive to a layer of particles with low coverage on top of the bilayer.

Here the value of using a deuterated lipid can be seen, as there would be minimal changes in the head group region of the bilayer by the incorporation of GMO, because the scattering length density of the head groups of DOPC and GMO are similar. However, deuteration of the acyl chains of the phospholipid makes it possible to observe this phenomenon. It is possible to estimate the scattering length densities of the head groups and acyl chain regions of d-DOPC and GMO by calculating the scattering lengths and estimating the volume for each part of the molecule. Based on this information the surface coverage and composition in the mixed bilayer can be quantified assuming a mixed bilayer composed only of GMO and d-DOPC molecules, and constant water content. Fig. 8 shows the results from this calculation together with the corresponding changes in thickness of the acyl chain region of the lipid bilayer *versus* time. The thickness of the acyl chain region is constant within the error bars after addition of the CPNPs, while the scattering length density decreases with time after injection of the nanoparticles. These

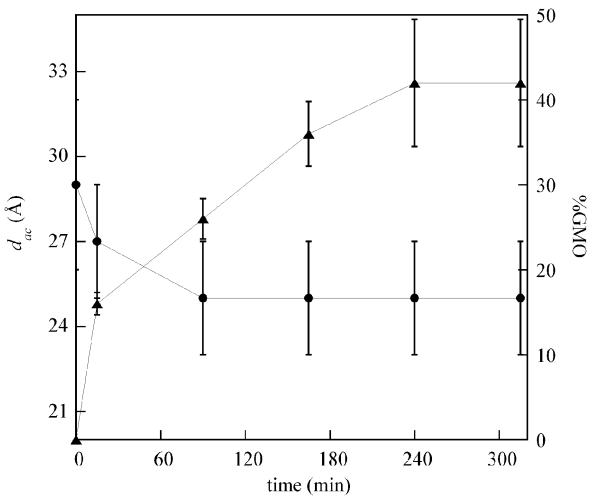

Fig. 8 Thickness of the acyl chain region (circles) and percentage of GMO present in the bilayer structure (triangles) determined by neutron reflectivity as a function of time after the addition of 0.001 mg ml^{-1} CPNPs to a d-DOPC bilayer at pH 4. The lines are shown as a guide to the eye only.

observations show unequivocally that there is exchange of material between the CPNPs and the lipid bilayer.

The solution concentration was then increased by addition of 0.05 mg ml^{-1} CPNPs at pH 4, and after 12.5 hours reflectivity profiles were recorded both in D_2O and in cmSi. This method allows the characterisation of the layer structure after the net release of material observed in ellipsometry. Fig. 9 shows the reflectivity profile of the layer in both isotopic solution contrasts.

The main feature of these curves is the appearance of a diffraction peak at high Q, which is evidence for an extended, ordered structure normal to the surface. A similar observation of an ordered surface phase has been made for lung surfactants, where phospholipids are the main constituents, at the air–water interface[42] and in the case of fluid DPPE bilayers.[43] This diffraction peak could not be fitted using a three-layer adsorption model, but could be fitted using a model with a stack of bilayers (composed mainly of GMO) appended to a first bilayer (mixed d-DOPC and GMO) adsorbed on the surface. Table 3 shows the parameters obtained for the absorbed layer at the end of the experiment, as compared to the initial DOPC bilayer and the mixed bilayer formed after interaction with the low concentration of CPNPs. The roughness of each layer in the multilayer was taken as 20% of the layer thickness. A resolution of 6% ($\Delta Q/Q$) was used in fitting the data.

The thickness and water content of the lipid bilayer increase, and the result is a bilayer with ~72% water. This observation suggests that after strong interaction with the CPNPs, the bilayer is partially consumed and the silica surface is depleted of DOPC. The process might be regarded as a dewetting of the lipid liquid crystalline phase on the silicon oxide surface. The water content of the multilayer structure is also very high, as indicated by the high value of the area per head group, which corresponds to coverage of particles after triggered release of ~18%.

The adsorbed layer on the surface thus comprises sparsely covered GMO-based particles with internal molecular organisation adhered to patches of mixed GMO–DOPC bilayer.

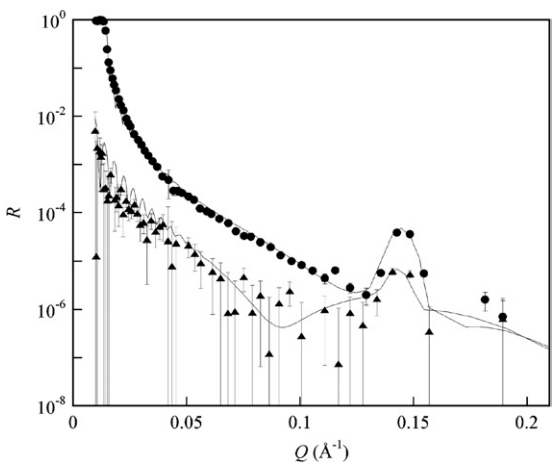

Fig. 9 Neutron reflectivity profiles recorded after the addition of CPNPs at a final concentration of 0.05 mg ml^{-1} after 12.5 h in D_2O (circles) and in cmSi (triangles) at pH 4. The lines correspond to the fitted curves obtained using a multilayer model appended to a bilayer next to the silica surface. Error bars for the D_2O measurements are in black and for cmSi measurements in grey.

Table 3 Neutron reflectivity fitting parameters for a d-DOPC bilayer (0 min) and for adsorbed layers after the interaction of 0.001 mg ml^{-1} and 0.05 mg ml^{-1} CPNPs. Notation is described in Table 2. Note that in this case ρ is taking into account the $\%_{solv}$ in the layer. N is the number of repeats in the multilayer structure and a_{hg} the area per head group. The roughness for the bilayer is kept the same as the value used previously

Bilayer properties	d_{hg}/Å	d_{ac}/Å	$\rho_{hg}/10^{-6}$ Å^2	$\rho_{ac}/10^{-6}$ Å^2
Bilayer	7 ± 1	29 ± 3	3.6 ± 0.2	6.2 ± 0.3
0.001 mg ml^{-1}	6 ± 1	25 ± 2	4.3 ± 0.2	4.7 ± 0.3
0.05 mg ml^{-1}	8 ± 1	32 ± 3	5.2 ± 0.2	5.6 ± 0.3

Multilayer properties	d_{hg}/Å	d_{ac}/Å	N	a_{hg}/Å^2
0.05 mg ml^{-1}	8.0 ± 0.3	27.5 ± 0.5	65 ± 5	320 ± 10

Comparison with the results from other techniques is difficult as the bilayer coverage is different. This issue will be addressed in detail in a study of the interaction of the CPNPs with bilayers of varying coverage.[44] Nevertheless, neutron reflectivity has shown that the composition of the DOPC bilayer changes upon interaction with the CPNPs. A 34% reduction in the amount of DOPC in the first bilayer (next to silica) after interaction with the high concentration of CPNPs shows conclusively that not only has there been adsorption of GMO to the bilayer, but that there has been loss of DOPC to the nanoparticles. These observations build on the conclusions drawn from ellipsometry and QCM-D measurements to provide a vivid mechanistic picture of the interaction: nanoparticle adsorption, lipid exchange and triggerable release.

Conclusions

Cubic phase nanoparticles are under development as drug delivery aids. In this work, we have shown that glycerol monooleate-based nanoparticles exhibit interesting interfacial behaviour of high relevance to the stated application. There is a strong interaction between the particles and a lipid bilayer. The particles adsorb to the lipid and exchange of material takes place. Increasing the solution concentration beyond a critical value can trigger release of the particles, which is rationalised in terms of sufficient incorporation of glycerol monooleate into the bilayer to switch the interaction from favourable to unfavourable. Hours after the addition of particles, the layer formed is constituted of a mixed bilayer with high water content with a low coverage of particles adhered to it.

Ellipsometry has shown clearly that the release of material from the surface, after the nanoparticles adsorb to the lipid bilayer, can be triggered through adjusting the solution concentration. Quartz crystal microbalance with dissipation monitoring has shown that once the system has reached steady state after the release of mass, the layer formed is highly viscoelastic, indicating that a low coverage of particles remained attached even hours after the initial interaction. Neutron reflectivity has provided valuable quantitative compositional information, and has shown that lipid exchange takes place between the two surface components. We use this result to explain the release of material from the interface in terms of decreasing favourability of nanoparticle fusion to the mixed lipid bilayer. The approach of applying

multiple experimental techniques to help the understanding of a very complex interfacial problem has been strongly validated.

Acknowledgements

This work is performed in the "New Principles for Oral Delivery of Peptides and Peptidomimetics" program. The Swedish Foundation for Strategic Research, Vinnova and Camurus Lipid Research Foundation financially supported this project as well as the Swedish Research council and its Linnaeus grant "Organizing Molecular Matter", OMM. We acknowledge Dr Daiva Tauraité, Vilnius University, Lithuania and Dr Chu Chuan Dong, University of Oxford who synthesised DOPC with deuterated acyl chains. The authors are grateful to the Institut Laue-Langevin, Grenoble, France for allocation of beam time for the neutron reflectivity measurements.

References

1 (*a*) K. Larsson, *Lipids – molecular organization, physical functions and technical applications*, The Oily Press Ltd, Dundee, 1994; (*b*) K. Larsson, P. Quinn, K. Sato and F. Tiberg, *Lipids – structure, physical properties and functionality*, The Oily Press Ltd, Dundee, 2006.
2 T. Norling, P. Lading, S. Engstrom, K. Larsson, N. Krog and S. S. Nissen, *J. Clin. Periodontol.*, 1992, **19**, 687–692.
3 L. Appel, K. Engle, J. Jensen, L. Rejewski and G. Zentner, *Pharm. Res.*, 1994, **11**, S217.
4 L. S. Nielsen, L. Schubert and J. Hansen, *Eur. J. Pharm. Sci.*, 1998, **6**, 231–239.
5 C. J. Drummond and C. Fong, *Curr. Opin. Colloid Interface Sci.*, 2000, **4**, 449–456.
6 J. C. Shah, Y. Sadhale and D. M. Chilukuri, *Adv. Drug Delivery Rev.*, 2001, **47**, 229–250.
7 F. Caboi, G. S. Amico, P. Pitzalis, M. Monduzzi, T. Nylander and K. Larsson, *Chem. Phys. Lipids*, 2001, **109**, 47–62.
8 P. Rowinski, A. Korytkowska and R. Bilewicz, *Chem. Phys. Lipids*, 2003, **124**, 147–156.
9 H. Chung, J. Kim, J. Y. Um, I. C. Kwon and S. Y. Jeong, *Diabetologia*, 2002, **45**, 448–451.
10 T. Landh and K. Larsson, *US Pat.*, 5 531 925, 1996.
11 K. Larsson, *Curr. Opin. Colloid Interface Sci.*, 2000, **5**, 64–69.
12 J. Barauskas, M. Johnsson and F. Tiberg, *Nano Lett.*, 2005, **5**, 1615–1619.
13 J. Barauskas, M. Johnsson, F. Joabsson and F. Tiberg, *Langmuir*, 2005, **21**, 2569–2577.
14 P. Vandoolaeghe, F. Tiberg and T. Nylander, *Langmuir*, 2006, **22**, 9169–9174.
15 E. Sackmann, *Science*, 1996, **271**, 43–48.
16 R. P. Richter, R. Berat and A. R. Brisson, *Langmuir*, 2006, **22**, 3497–3505.
17 F. Tiberg, I. Harwigsson and M. Malmsten, *Eur. Biophys. J. Biophys. Lett.*, 2000, **29**, 196–203.
18 S. T. Hyde, S. Andersson, B. Ericsson and K. Larsson, *Z. Kristallogr.*, 1984, **168**, 213–219.
19 H. Qui and M. Caffrey, *Biomaterials*, 2000, **21**, 223–234.
20 D. M. Anderson, S. M. Gruner and S. Leibler, *Proc. Natl. Acad. Sci. U. S. A.*, 1988, **85**, 5364–5368.
21 D. C. Turner, Z. G. Wang, S. M. Gruner, D. A. Mannock and R. N. Mcelhaney, *J. Phys. II*, 1992, **2**, 2039–2063.
22 F. Tiberg and M. Landgren, *Langmuir*, 1993, **9**, 927–932.
23 M. Landgren and B. Jonsson, *J. Phys. Chem.*, 1993, **97**, 1656–1660.
24 L. M. Grant and F. Tiberg, *Biophys. J.*, 2002, **82**, 1373–1385.
25 H. P. Vacklin, F. Tiberg and R. K. Thomas, *Biochim. Biophys. Acta*, 2005, **1668**, 17–24.
26 H. P. Vacklin, F. Tiberg, G. Fragneto and R. K. Thomas, *Langmuir*, 2005, **21**, 2827–2837.
27 P. Petrov, *Ellipsometry, v. 1.3.1*, 1994–2001.
28 F. L. McCrackin and J. P. Colson, *Natl. Bur. Stand. (US), Misc. Publ.*, 1964, **256**, 61–82.
29 F. L. McCrackin, E. Passaglia, R. R. Stromberg and H. L. Steinberg, *J. Res. Natl. Bur. Stand. (US)*, 1963, **67A**, 363–377.
30 T. E. Jenkins, *J. Phys. D: Appl. Phys.*, 1999, **32**, R45–R56.
31 J. A. Defeijter, J. Benjamins and F. A. Veer, *Biopolymers*, 1978, **17**, 1759–1772.
32 J. Campos, K. Eskilsson, T. Nylander and A. Svendsen, *Colloids Surf., B*, 2002, **26**, 172–182.
33 M. Rodahl, F. Hook, C. Fredriksson, C. A. Keller, A. Krozer, P. Brzezinski, M. Voinova and B. Kasemo, *Faraday Discuss.*, 1997, **107**, 229–246.
34 M. V. Voinova, M. Rodahl, M. Jonson and B. Kasemo, *Phys. Scr.*, 1999, **59**, 391–396.
35 R. Cubitt and G. Fragneto, *Appl. Phys. A: Mater. Sci. Process.*, 2002, **74**, S329–S331.
36 S. F. Turner, S. M. Clarke, A. R. Rennie, P. N. Thirtle, D. J. Cooke, Z. X. Li and R. K. Thomas, *Langmuir*, 1999, **15**, 1017–1023.
37 S. F. Turner, PhD thesis, University of Cambridge, 1998.
38 J. R. Lu and R. K. Thomas, *J. Chem. Soc., Faraday Trans.*, 1998, **94**, 995–1018.
39 M. Born and E. Wolf, *Principles of Optics*, Cambridge University Press, Cambridge, 7th edn, 1999.
40 P. N. Thirtle, *AFit Simulation Program*, Oxford University, 1997.
41 C. A. Keller and B. Kasemo, *Biophys. J.*, 1998, **75**, 1397–1402.
42 D. Follows, F. Tiberg, R. K. Thomas and M. Larsson, *Biochim. Biophys. Acta*, 2007, **1768**, 228–235.
43 B. Stidder, G. Fragneto and S. J. Roser, *Soft Matter*, 2007, **3**, 214–222.
44 P. Vandoolaeghe, A. R. Rennie, R. A. Campbell and T. Nylander, *Langmuir*, submitted.